Low-temperature magnetism of quinolinium$(TCNQ)_2$, a random-exchange Heisenberg antiferromagnetic chain. II. Dynamic properties

L. C. Tippie and W. G. Clark
Department of Physics, University of California at Los Angeles, Los Angeles, California 90024
(Received 8 July 1980)

Several experiments on the dynamic properties of the electron spins in quinolinium-di-tetracyanoquinodimethanide are reported. They include pulsed electron spin resonance (ESR) over the frequency (ν) and temperature (T) ranges 241–400 MHz and 0.04–4.2 K, as well as cw ESR over the ranges 10–290 MHz and 0.03–300 K. Both polycrystalline and single-platelet samples were investigated. In all of the cw experiments, a single, narrow, Lorentzian line shape is observed. It is shown that this is a result of narrowing of dipolar and hyperfine interactions by an undetermined combination of isotropic-exchange and electron-spin-delocalization effects. At low T the ESR linewidth $\Delta H_{1/2}$ has a slow logarithmic divergence with decreasing ν and T. The pulsed ESR experiments include spin-echo measurements of the transverse spin-phase memory time (T_{2e}), and the recovery of the longitudinal magnetization. Below 100 mK, the latter displays both a fast (T_{1e}) and a slow (τ_B) recovery time. Typical values for T_{1e} and T_{2e} are 1 μs and 0.5 μs, respectively, and both vary weakly with ν and T. It is proposed that T_{1e} represents relaxation between the Zeeman and exchange reservoirs. At 50 mK, $\tau_B = 7$ ms, and varies as $\tau_B \propto T^{-4\pm1}$. It is attributed to relaxation of the Zeeman and exchange reservoirs to the He bath, and may be determined by the Kapitza resistance. These results are further evidence that quinolinium$(TCNQ)_2$ is a random-exchange Heisenberg antiferromagnetic chain.

I. INTRODUCTION

A substantial amount of recent work on the magnetic properties of quinolinium-di-tetracyanodimethanide [quinolinium$(TCNQ)_2$] has the characteristics of a random-exchange Heisenberg antiferromagnetic chain (REHAC) with spin $S = \frac{1}{2}$. This interpretation is supported by measurements of the magnetization[1,2] (M), magnetic susceptibility[3–6] (χ), and specific heat[7] (C_H) at constant magnetic field (H). These experiments probe the static properties of the magnetic chains. In this paper, we present and interpret measurements of their dynamic properties using cw and pulsed electron spin resonance (ESR) over a wide range of temperature. Our work on the static properties appears in the paper immediately preceding this one.[3]

Two types of experiments have already been reported which are related to the dynamics of these systems. The first is relaxation of the proton spins by electron-spin fluctuations.[8,9] Significant progress has been made in the interpretation of these results in the regime where the electron Zeeman splitting is less than k_BT (k_B is Boltzmann's constant and T is the temperature) using one-dimensional diffusion models for the motion of the electron spin.[10] On the contrary, there is still no detailed explanation for the unusual behavior reported[9] at temperatures low enough that the electron Zeeman splitting is on the order of or large compared to k_BT. The second reported measurement of electron spin dynamics in quinolinium$(TCNQ)_2$ is the ESR linewidth.[11] In this case, we are also not aware of any quantitative interpretation of the experimental observations.

In the work reported here, a more direct approach to the spin dynamics is employed. The longitudinal and transverse relaxation of the electron spins are measured using the techniques of pulsed electron spin resonance. In addition, the cw ESR linewidth is reported. To the best of our knowledge, the relaxation measurements presented here are the first direct measurements of the dynamic behavior of the electron spins in a REHAC.

The transient quantities measured in our experiments are the recovery time of the electron spin magnetization parallel to H after it has been disturbed from equilibrium by an rf pulse and the spin-phase memory time using spin echoes. The frequency (ν) temperature ranges covered are respectively $241 < \nu < 400$ MHz and 40 mK $< T <$ 4.2 K, which corresponds to $86 < H < 143$ Oe. The linewidth (half width at half maximum, $\Delta H_{1/2}$) is reported for frequencies ranging from 10 MHz (3.6 Oe) to 290 MHz (103 Oe) and temperatures over the range 30 Mk $< T <$ 300 K. The experimental results are presented in Sec. III, following a description of exper-

imental details in Sec. II. Preliminary reports of this have been published elsewhere.[6,12]

One of our major results is that the recovery of the longitudinal magnetization has two components. One of them is fast (~ 1 μs) and nearly independent of T over a range $\sim$100:1 in T. The other component is much slower and strongly ($\sim T^{-4}$) dependent on T. In Sec. IV these properties are interpreted using a two-reservoir (exchange and Zeeman) model for the exchange of energy between the magnetic degrees of freedom. This picture is consistent with the behavior expected of a REHAC. Since there is not yet any theory for calculating the appropriate relaxation rates and $\Delta H_{1/2}$ in a REHAC, our interpretation of these points in Sec. IV is qualitative, and found to be consistent with the properties of a REHAC.

II. EXPERIMENTAL DETAILS

The samples used in this work were provided by K. Holczer of the Central Research Institute for Physics, Budapest, A. J. Heeger of the University of Pennsylvania, and N. Rysava of the Institute of Physics, Prague. They are labeled 1, 2, and 3, respectively. They were prepared using standard synthesis techniques and, where tested, showed properties recognized as characteristic of quinolinium(TCNQ)$_2$. Other low-temperature magnetic measurements on these samples have been reported elsewhere; in particular, the specific heat[7] of sample 1 (whose characteristics are discussed in more detail there) and the static susceptibility of all three.[3]

Most of the work reported here was done on $\sim$5 mg polycrystalline samples which were lightly compressed into thin-walled quartz tubes. Quartz was used to avoid the spurious ESR signal found in Pyrex. The magnetic resonance coil was wound on the outside of the quartz tube. A few linewidth measurements as a function of field orientation were made on a single platelet measuring approximately 2 μm $\times$ 8 μm $\times$ 2 mm ($\sim$0.05 μg of material). In this case a freely suspended coil made from 13-μm-diameter insulated Cu wire and having 60 turns and an inside diameter of 25 μm was used. This coil was wound on a thin (25 μm) wire form. After winding, the form was removed and the sample carefully slid into place. Even though the coil was unusually small, the sample was still much smaller, so that the filling factor was quite low ($\sim$0.03). Nevertheless, viable signals could be obtained with this arrangement.

Cooling below 4.2 K was achieved via direct contact with He vapor or liquid in the mixing chamber of a dilution refrigerator. A calibrated carbon resistor was used for thermometry. Above 4.2 K T was controlled with a gas-flow system and measured with a Ge resistance thermometer. In both cases, the uncertainty in T was 2% or less.

Longitudinal and transverse electron spin relaxation times were measured using a low power, pulsed magnetic resonance spectrometer[13] operating over the frequency range 240–400 MHz. Standard pulse sequences, such as those used for pulsed NMR, were employed. Longitudinal relaxation was observed using a pair of equal angle pulses and registering the amplitude of the free-induction decay following the second pulse as a function of the time interval between the pulses. Transverse relaxation was measured with a pair of pulses the first of which was twice the length of the second, and recording the amplitude of the spin echo as a function of pulse separation. Ideally, the pulse sequences for these experiments would be 90°-90° and 180°-90°. Because of the low power available with the spectrometer, the pulse lengths were on the order of the free-induction-decay time (T_{2e}^*), with the consequence that there was an appreciable uncertainty in the actual angles through which the magnetization was tipped. The pulses were usually set to maximize the signal available for each measurement. With our conditions of low rf power, short T_2^*, and the recovery time mentioned below, maximizing the signal usually meant tipping the magnetization through smaller than normal angles.

Even though over the temperature range (40 mK–4.2 K) investigated the ESR line is rather narrow (0.1–0.25 G), T_{2e}^* and relaxation times were quite short ($\sim 10^{-7}$ to 10^{-6} s). The dead time of the spectrometer was reduced to $\sim$0.5 μs, which was sufficient to produce acceptable signals. Representative errors are indicated with the data.

Steady-state linewidth measurements of $\Delta H_{1/2}$ at frequencies greater than 200 MHz were performed using a high-frequency Q-meter absorption spectrometer,[13] field modulation, and lock-in detection. The derivative signal thus obtained was integrated to give the absorption signal. At frequencies below 200 MHz the linewidth was obtained via direct recording of the absorption signal upon sweeping the field using a different low-level Q-meter absorption spectrometer.[14]

Measurements of linewidth as a function of field orientation were done by keeping the sample fixed in the mixing chamber and changing the field direction.

III. EXPERIMENTAL RESULTS

In this section we present the experimental results. Their interpretation is given in the next section. First the transient measurements are described, followed by the steady-state ones.

The recovery of the longitudinal magnetization (M_z) is shown in Fig. 1. There, it is seen that about 90% of the recovery time at 48 mK is very fast (see inset) with a characteristic time constant of about 1 μs followed by a much slower recovery whose charac-

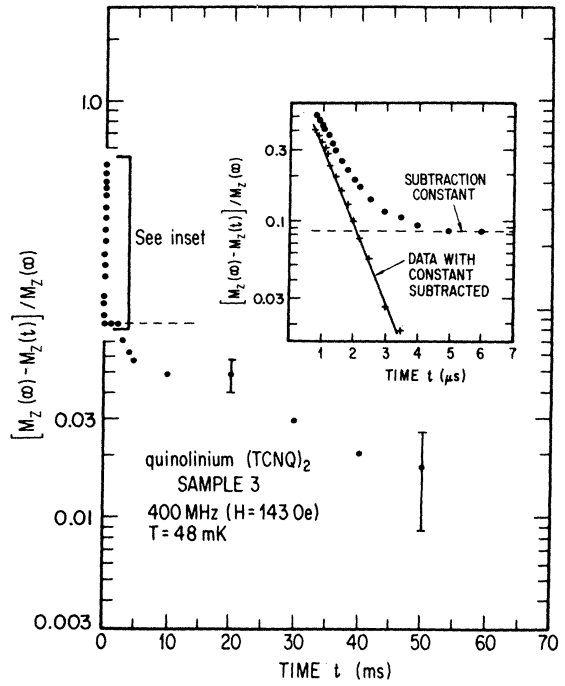

FIG. 1. Recovery of the longitudinal magnetization as a function of time at 48 mK. The inset shows the fast component in more detail. It is attributed to Zeeman-exchange relaxation, and the slow recovery is associated with the relaxation of both reservoirs to the bath.

teristic time is about 10^{-2} s. Since the two time scales are so different, the corresponding parts are easily separated, as shown in the inset of Fig. 1. The fast recovery is exponential (time constant T_{1e}), whereas the slow recovery is more complicated. The exponential form of the fast recovery is shown by the straight line in Fig. 1. On Fig. 2, data showing the

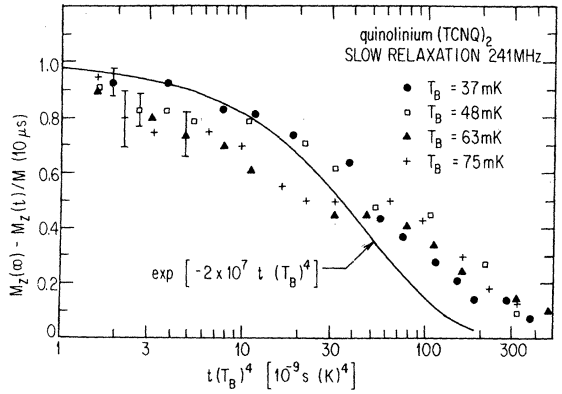

FIG. 2. Recovery of the slow component of the magnetization of sample 3 as a function of time for several different temperatures. The time axis is normalized by T_B^4 to show that, although the form of the slow recovery is not exponential (solid line), it has the same shape at different temperatures and varies approximately as T^{-4}.

form of the slow recovery are shown for several different values of T. For reasons to be made clear later, the time scale is multiplied by T_B^4, where T_B is the temperature of the bath. The departure of the slow recovery from exponential form is seen by comparison of the data with the exponential indicated by the solid line. This separation of the recovery into a fast exponential part followed by a slow recovery of more complicated form occurs only in the low T range, and the lower T is, the more pronounced is the slow recovery. Within the accuracy of our measurements, only the fast recovery is observed above 100 mK.

The decay of the transverse magnetization at 40 mK as measured in the spin echo experiments is shown in Fig. 3. At each T a single exponential is observed, thereby giving a unique spin-phase memory time T_{2e}.

Values of T_{1e} and T_{2e} over a wide range of T at several values of ν are shown in Figs. 4 and 5, respectively. In addition, T_{2e}^* calculated from $\Delta H_{1/2}$ is shown on Fig. 5. The experimental values of T_{1e} and T_{2e} obtained at any given T depend weakly on the pulse angles used. Our maximum observed variation is about ±8%, and is the main contribution to the experimental uncertainty indicated by the error bars. A given pulse sequence gives an uncertainty in recovery time which is somewhat less, about 3–8%. The central fact evident from Figs. 4 and 5 is that over a range of 100:1 in T for T_{1e} and a smaller factor of 10 for T_{2e}, these relaxation times are nearly independent of T.

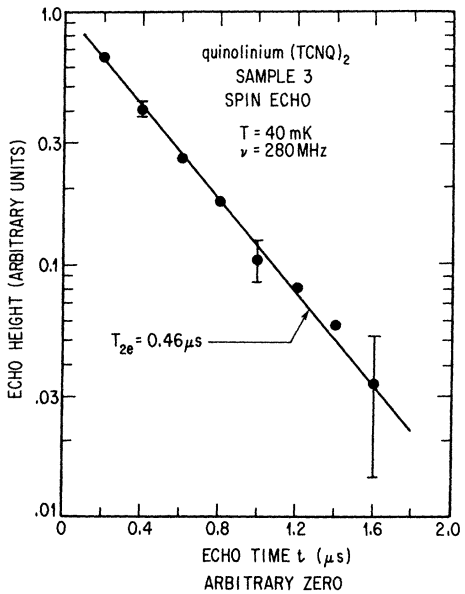

FIG. 3. Spin-echo decay as a function of time.

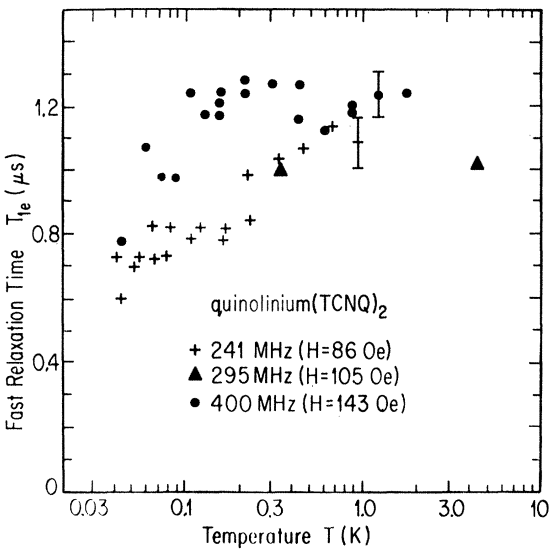

FIG. 4. Fast relaxation time of sample 3 as a function of T at several frequencies. The weak dependence of T and ν is used to identify the process as magnetic cross relaxation between the Zeeman and exchange reservoirs.

In contrast to the fast relaxation, the slow relaxation has a strong T dependence. This is indicated on Fig. 2, where it is seen that scaling T by T_B^4 gives a form to the relaxation which is nearly independent of T_B. Although the shape of the recovery curve is not exponential, there is characteristic time for the slow recovery to go halfway to its final value (τ_B) which has the same meaning for all T. It is shown in Fig. 6

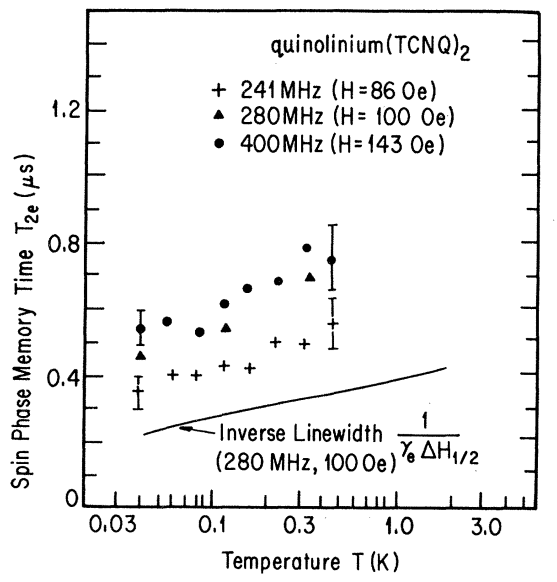

FIG. 5. Spin phase memory time and inverse linewidth of a polycrystalline compaction of sample 3 as a function of temperature.

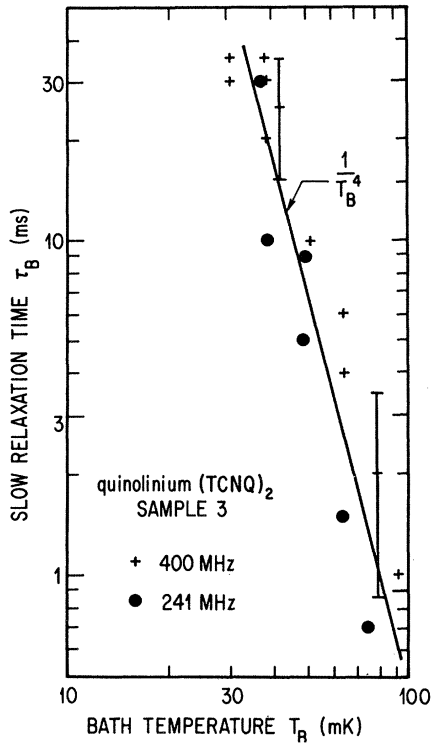

FIG. 6. Slow relaxation time as a function of temperature at two frequencies. The strong T dependence may be determined by the Kapitza resistance of the sample.

at two frequencies as a function of T_B using logarithmic scales. There it is seen that τ_B varies approximately as T^{-4} (we estimate $\tau_B \propto T^{-(4.0\pm1.0)}$).

Next, we present our cw ESR absorption line shapes. Although not all of our recorded ESR lines have been analyzed for their shape, many of them have been checked covering all of the conditions representative of our measurements. In no case has a significant deviation from a Lorentzian shape been observed. Visual inspection of the rest shows them all to have the features characteristic of a Lorentzian shape. We therefore conclude that all of the conditions covered in our experiments generate Lorentzian ESR absorption lines.

Our measurements were made on both polycrystalline samples consisting of many platelets oriented at random and a single-platelet sample. First, we consider the polycrystalline samples. The linewidth $\Delta H_{1/2}$ at several frequencies over the temperature range $0.03 < T < 300$ K for samples 1 and 2 is shown in Figs. 7 and 8, respectively. It drops from about 0.15 G to a minimum of about 0.05 G at 25 K and then slowly rises as the temperature is lowered further. The onset of this low-temperature rise also coincides with the beginning of the low-temperature exponent behavior of the magnetic susceptibility χ observed in these samples.[3] At $\nu = 42$ MHz and

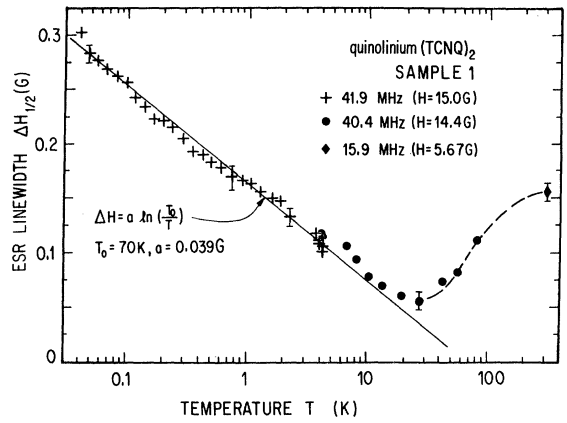

FIG. 7. ESR linewidth of a polycrystalline sample as a function of T. The logarithmic increase at low T may be due to increased localization of the electron spins and the reduction of exchange narrowing at low T.

below, the low-temperature behavior of these two samples is similar, but not identical. The low-temperature data of sample 1 follow rather closely the empirical relation

$$\Delta H_{1/2} = 3.9 \times 10^{-2} \ln\left(\frac{70\ \text{K}}{T}\right) \text{G} \ . \qquad (1)$$

In Fig. 9 the dependence of $\Delta H_{1/2}$ on ν at $T = 42$ mK is shown for sample 1. There, it is seen that below $\nu = 100$ MHz, H increases slowly with decreasing frequency according to the empirical relation

$$\Delta H_{1/2} = 0.63 \times 10^{-1} \ln\left(\frac{5.13\ \text{GHz}}{\nu}\right) \text{G} \ . \qquad (2)$$

Above 200 MHz, $\Delta H_{1/2}$ starts to rise, perhaps to the same value reported[2] at 9.5 GHz.

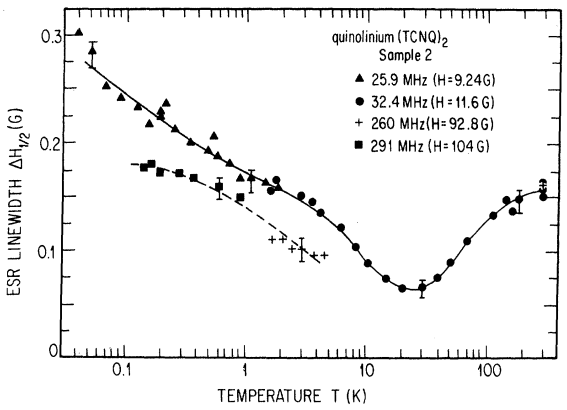

FIG. 8. ESR linewidth as a function of T for (polycrystalline) sample 2 at several frequencies. The solid and dashed lines are a guide to the eye.

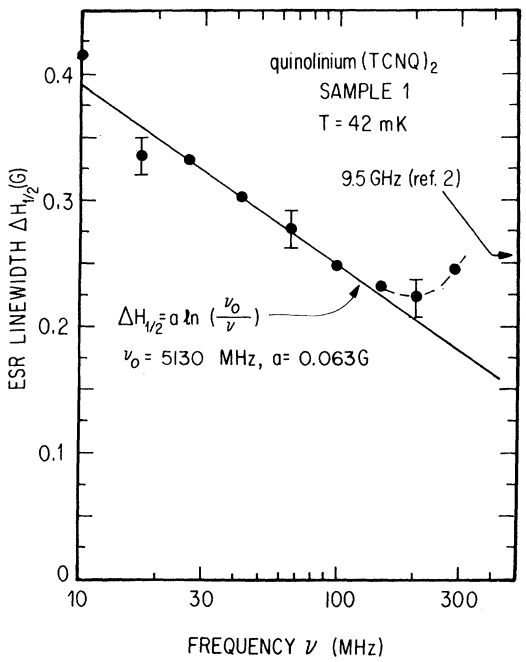

FIG. 9. ESR linewidth of a polycrystalline sample as a function of ν at 42 mK. The linewidth 0.26 G for a single needle at 9.5 GHz and extrapolated to 42 mK (Ref. 2) is also indicated.

Measurements of $\Delta H_{1/2}$ as a function of field orientation are shown for a single platelet of sample 3 in Figs. 10–12. The z axis was taken as the chain axis (the longest direction of the platelet), and the x and y axes to form an orthogonal basis with the y axis perpendicular to the largest face. Rotations were made in three orthogonal planes as follows: First a rotation was made in the xy plane (Fig. 10) to identify the directions giving maximum and minimum values of $\Delta H_{1/2}$. These directions were found to be 30° beyond the x and y axes as shown. Subsequent rotations (Figs. 11 and 12) were made in planes containing the z axis and the directions corresponding to the maximum and minimum of Fig. 10. For definitions of the various angles refer to the figures.

The needle chosen had well-defined faces when viewed under magnification. It is not known, however, if this platelet was a single crystal. The frequency of measurement, 56.5 MHz, was not high enough to use the anisotropy of the g-value[6] as a test of this point. On the other hand, the large anisotropy with a simple two-fold symmetry suggests that the sample was, in fact, a single crystal.

There is a complication in comparing Figs. 10–12: Figs. 11 and 12 were obtained at 79 mK, whereas the 45 mK indicated for Fig. 10 is a lower limit; the actual temperature may have been as much as a few mK above this. The reason for this is that there was a

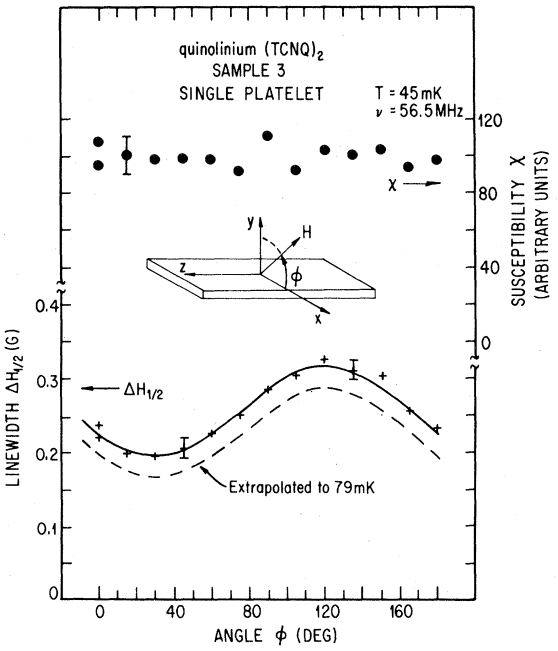

FIG. 10. ESR linewidth of a single platelet as a function of field orientation for $\vec{H}$ perpendicular to the chain axis. For comparison with other results, Fig. 7 has been used to extrapolate to 79 mK. The solid line is a guide to the eye and the dashed line is Eq. (3).

slight amount of rf heating for Fig. 10 and none for the others. The amount of heating was the same for all the data of Fig. 10. This was verified by measuring the area under the absorption curve at each angle. It is plotted as χ as a function of ϕ (solid circles, right hand axis) on Fig. 10, and shows that the integrated intensity, and therefore the temperature, was the same for all of the points.

It is easy to extrapolate the 45 mK data of Fig. 10 to the 79 mK of Figs. 11 and 12. The minima of

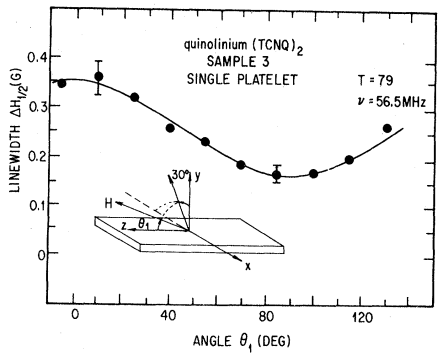

FIG. 11. ESR linewidth of a single platelet as a function of field orientation in a plane containing the chain axis. The solid line is a plot of Eq. (4).

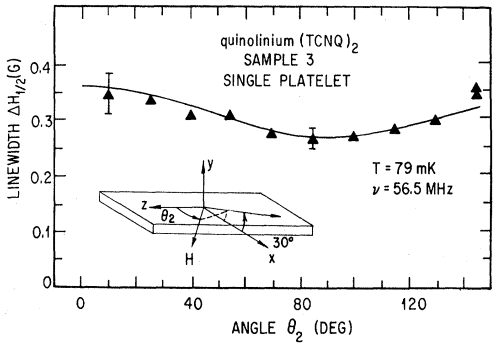

FIG. 12. ESR linewidth of a single platelet as a function of field orientation in a plane containing the chain axis. The solid line is a plot of Eq. (5).

Figs. 11 and 12 correspond, respectively, to the same directions as the minimum and maximum of Fig. 10. Inspection of these figures shows that Fig. 9 can be brought into coincidence with Figs. 11 and 12 by simply subtracting 0.03 G from all values of $\Delta H_{1/2}$ on Fig. 10. This is shown by the dashed line on Fig. 10. It is very close to the correction (0.025 G) which one would infer from Fig. 7.

The curves used to fit $\Delta H_{1/2}$ (determined from a least-squares fit) at 79 mK for the various rotations are:

$$\text{(Fig. 10)}\ \Delta H_{1/2} = [0.125\cos^2(\phi + 60°) + 0.195]\ \text{G}\ , \tag{3}$$

$$\text{(Fig. 11)}\ \Delta H_{1/2} = (0.189\cos^2\theta_1 + 0.167)\ \text{G}\ , \tag{4}$$

$$\text{(Fig. 12)}\ \Delta H_{1/2} = (0.086\cos^2\theta_2 + 0.270)\ \text{G}\ . \tag{5}$$

It is seen that for all the orientations tested, H parallel to the chain axis corresponds to the largest $\Delta H_{1/2}$.

IV. INTERPRETATION

In this section we analyze and discuss the data presented in Sec. III.

A. Longitudinal relaxation

The main features in the relaxation of M_z are the following: Below 0.1 K, two components of relaxation are seen, a fast one and a slow one (Fig. 1). The fast one is exponential (Fig. 1), almost independent of temperature between 0.04 and 4.2 K (Fig. 4), and only weakly dependent on frequency between 0.04 and 4.2 K. The slow relaxation is strongly temperature dependent below 0.1 K (Fig. 6), nonexponential (Fig. 2), and not observed above 0.1 K.

Here, we present a model which we believe con-

tains the correct physical explanation for the behavior of M_z. It is based on three weakly coupled thermal reservoirs, as indicated in the upper part of Fig. 13. They are the Zeeman reservoir, with a Hamiltonian

$$H_Z = -g\mu_B H \sum_i S_i^z \tag{6}$$

and temperature T_Z, the exchange reservoir, with a Hamiltonian

$$H_E = 2 \sum_i J_i \vec{S}_i \cdot \vec{S}_{i+1} \tag{7}$$

and temperature T_E, and the helium bath, for which an infinite heat capacity and constant temperature T_B are assumed. In Eqs. (6) and (7), i is the site index on the one-dimensional chain of spins, $\vec{S}_i$ is the spin operator ($S = \frac{1}{2}$) of the ith site, and J_i is the nearest-neighbor antiferromagnetic ($J > 0$) exchange interaction, which is random with a distribution function $P(J)$. Models of this type have been used repeatedly to explain the relaxation behavior of electron spins coupled by exchange and other interactions,[15] and even for nuclei in solid ^{3}He.[16]

The Hamiltonian $H = H_E + H_Z$ has been widely used to explain the static magnetic properties of

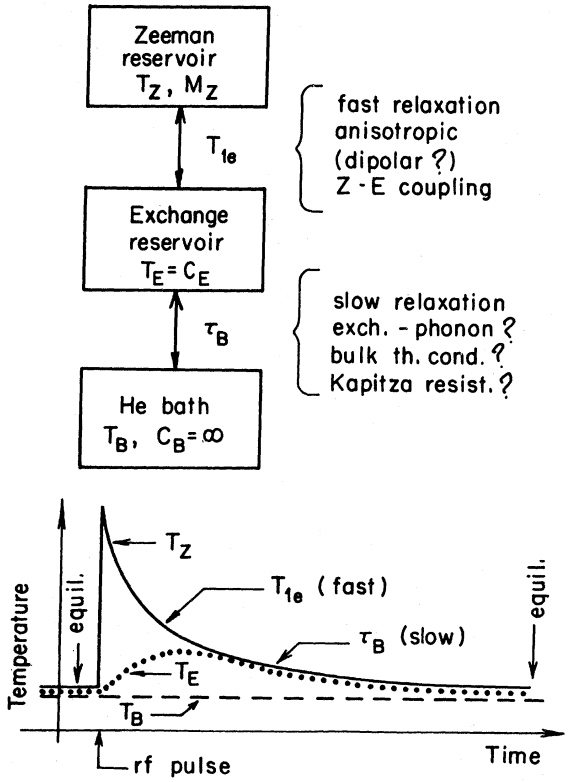

FIG. 13. Block diagram for the reservoir model used to explain T_{1e} and τ_B (upper part). Schematic graph of T_2 and T_e as a function of t at low T in a pulsed ERS experiment (lower part).

quinolinium(TCNQ)$_2$. For example, H_E is responsible for the zero-field specific heat[7] [$C_H(0,T)$], which varies as

$$C_H(0,T) = BT^{1-\alpha} \tag{8}$$

at low T. (The parameter α is a constant which appears in the various theoretical models.) Both H_E and H_Z combine to give the observed[3]

$$\chi = AT^{-\alpha} \tag{9}$$

at low H. These points are covered in detail elsewhere, where the Bulaevskii[1] model, the ECP model,[6,17,18] the cluster model of Theodorou and Cohen,[19] and the recent renormalization calculations are discussed.[20–22]

In order for H_E and H_Z to function individually as thermal reservoirs it is important that they not be strongly coupled to any other reservoir and that there be a means of establishing internal thermal equilibrium.[23] They are not coupled strongly together because $[H_E, H_Z] = 0$.

We *assume* that they have no strong interactions with other reservoirs, such as the phonons in the sample or the helium bath. In order to allow some energy flow between H_E, H_Z, and the bath, additional weak couplings among them are needed. They are also needed to explain the linewidth measurements discussed in the next section. The real system provides a large number of such couplings, some of which are the electron-electron dipolar interaction[24] (H_d), the isotropic (I) and anisotropic (A) electron-nuclear (hyperfine and dipolar) interactions, $^{24}H_{In}$ and H_{An}, and the exchange-phonon interaction[25] H_{ep}. The term H_d is especially important for the reservoir model of relaxation, as it may provide the weak coupling *between* reservoirs, which gives the observed relaxation, as well as provide a coupling *within* each reservoir, which is important for the establishment of an internal temperature. These properties of H_d can be shown for example, with the ECP model.[17]

Now consider the relationships between the three reservoirs and the observed behavior of M_z.[26] Before attempting to justify them, we give a qualitative description of what happens. This is illustrated in time sequence on the lower part of Fig. 13, where the various temperatures are sketched as a function of time (t). The quantity directly observed is the value of M_z just before an rf pulse is applied to the electrons. The amplitude of the signal is proportional to M_z. Since $M_z = \chi(T_Z)H$ and $\chi \propto T_Z^{-\alpha}$, observation of the signal amplitude constitutes a measurement of T_Z. Starting from thermal equilibrium ($T_E = T_Z = T_B$), the rf pulse is applied, which immediately increases T_Z. The subsequent fast (1 μs) relaxation time T_{1e} is interpreted as relaxation of the Zeeman and exchange reservoirs to a common intermediate temperature. Thus, on a time scale of 1 μs, the ESR signal also provides a measure of T_E. Below 0.1 K,

the slow relaxation time τ_B represents the relaxation of T_Z and T_E in unison to T_B.

There are several arguments to make plausible the near independence of T_{1e} on T and ν. Following standard transition probability theory,[27] T_{1e}^{-1} is proportional to $|H_d|^2$ for interacting pairs of spins, proportional to the number of possible transitions which conserve energy (density of states factor), and depends on the thermal populations of the states involved in the transitions. As demonstrated in our experiments, the spectral width of H_Z is narrow ($\sim\gamma_e \Delta H_{1/2}$) and centered about ν. On the other hand, the spectrum of energy levels of H_E is extremely broad, as exemplified by the experiments which support[7] Eq. (8). The relevant density of states is therefore determined mainly by H_E. As long as $g\mu_B H \ll k_B T$, none of these factors is expected to show a strong dependence on T or ν; hence neither should T_{1e}, in agreement with our experimental results. The process just described is a form of magnetic cross relaxation rate which is strongly influenced by the overlap in the states of H_E and H_Z. Phonons play no direct role in it.

We have not been able to translate these ideas into a quantitative calculation of T_{1e} for a REHAC. Part of the problem is that at low T there is not characteristic J in the problem. The range of J is so large (at least after renormalization[20–22]) that there are always a substantial number of values which are both large and small compared to both $k_B T$ and $g\mu_B H$. This large range in J and one dimensionality are two features which distinguish a REHAC from earlier treatment of Zeeman-exchange reservoir relaxation.[15,16]

There are two other observations about T_{1e} in quinolinium(TCNQ)$_2$ which help to identify it as due to Zeeman-exchange relaxation. The first is the rise in T_E at the end of the short time interval when T_E and T_Z have first reached a common T after an rf pulse, as measured by the fraction of the recovery ($\delta\chi/\chi$) represented by the slow mode. In Fig. 1, this fraction is seen to be 8.5% at 48 mK and $H = 143$ Oe. The rise in T_E can be estimated using simple energy balance arguments. The effect of the rf pulse is to reduce M_z from its equilibrium value $M_z(\infty)$ to $M_z(\infty)\cos\beta = \chi(T_B)H\cos\beta$, where β is the angle by which the pulse tips the magnetization from the z axis. When M_z relaxes back to $M_z(T_E)$ by the amount ΔM, a quantity of energy $E = (\Delta M)H \approx \chi(T_B)(1-\cos\beta)H^2$ is absorbed by H_E, which raises T_E by $\delta T_E \approx E/C_H(0,T_B)$. Since $\chi \propto T^{-\alpha}$, we have for small δT_E

$$\frac{\delta T_E}{T_E} = -\alpha\frac{\delta\chi}{\chi} \ , \tag{10a}$$

$$\frac{\delta T_E}{T_E} \approx \frac{(1-\cos\beta)(T_B)H^2}{C_H(0,T_B)T_B} \ . \tag{10b}$$

These equations can be compared with our experiment at $T_B = 48$ mK and $H = 143$ Oe by using $C_H(0, 48\text{ mK}) = 1.3\times10^5$ erg/mole K (extrapolated from measurements[7] to 70 mK on a sample with $\alpha = 0.82$, which is similar to our sample 3) and $\chi(48\text{ mK}) = 5.6\times10^{-2}$ cm^3/mole for sample 3, which has[3] $\alpha = 0.85$. Equation (10a) yields $\delta T_E/T_E = 10\%$, whereas if $\beta = 90°$, Eq. (10b) indicates $\delta T_E/T_E = 18\%$; if $\beta = 64°$, $\delta T_E/T_E = 10\%$, which is observed. As indicated in Sec. II, the angle β is not precisely determined in our experiments, but is probably somewhat less than 90°. Thus, δT_E just calculated is consistent with the idea that T_{1e} is due to Zeeman-exchange relaxation.

The other observation tending to substantiate this reservoir model is the disappearance of the slow relaxation above about 100 mK. The fraction of the whole recovery signal corresponding to the slow recovery is approximately $\delta T_E/T_E \propto H^2/T^2$. Since this scales as T^{-2}, going from 48 to 100 mK reduces the amplitude of the slow relaxation mode from 10% to only 2.5%, at which point it becomes difficult to observe.

There are several mechanisms for the common (slow) relaxation of the Zeeman and exchange reservoirs to the helium bath, which we associate with τ_B. The most conventional one has three steps in series: relaxation of the exchange reservoir to the phonons in the bulk of the sample, conduction of heat by the phonons from the bulk to the surface, the conduction of heat across the surface into the bath against the Kapitza resistance (R_B). Roughly speaking, since these operate in series, the overall time scale in the slow relaxation will be set by the weakest of the three processes acting as a bottleneck. The observation $\tau_B \propto T_B^{-4\pm1}$ indicates that the Kapitza resistance may be the limiting process, since the acoustic mismatch theory[28] and many experiments on other materials indicate $R_B \propto T^{-3}$ when the temperature difference across the boundary is small, and $R_B \propto T^{-4}$ when it is not. It is suggestive to estimate the thermal time constant $\tau_{th} = R_B C_H$ of a typical needle of quinolinium(TCNQ)$_2$ in ^{4}He at 50 mK. By using the typical dimensions $0.2\times10^{-4}\times4\times10^{-4}$ cm^3, density[29] $\rho = 1.4$ g/cm^3, specific heat[7] $C_H \cong 20$ μJ/g K, and typical boundary resistance coefficient[28] $r = (100/T^3)$ (K^4 cm^2/W) we obtain $\tau_{th} \simeq 0.8$ ms. The observed value (7 ms in Fig. 6) is an order of magnitude larger. However, given the uncertainties in such estimates, the Kapitza resistance remains a plausible candidate for the physical origin of τ_B. If this process is the determining factor, it could also explain the nonexponential recovery (Fig. 2) as due to the distribution in size of the platelets, which we have observed under magnification to be rather broad.

Although the above interpretation of $\tau_B \propto T^{-4\pm1}$ as coming from R_B is plausible, it should be accepted with caution as there are many factors whose impor-

tance to the relaxation has not been evaluated. They include estimates of the exchange-phonon relaxation rate, the possibility that transport to the surface of the platelet is carried by magnetic excitations rather than phonons, the possibility that relaxation occurs via direct magnetic coupling to ^{3}He in the mixing chamber,[30] the possibility that coupling out of the magnetic degrees of freedom is via the Zeeman rather than the exchange reservoir, and the possibility that there is heating of the bath in the vicinity of the sample. Another point which could be important for the energy transport in the system is the fact that the wavelength λ_{th} of a thermal phonon at the lowest T[31] is comparable to the smallest dimension (~ 1 μm) of a typical platelet.

B. ESR linewidth

In this discussion we focus attention mainly to the linewidth results below 20 K, where there is a substantial degree of localization of the electrons along the TCNQ chains.[32] The main experimental observations are: a single, narrow, Lorentzian line, a $\Delta H_{1/2}$ which increases slowly ($\sim$logarithmically) as T is decreased, a $\Delta H_{1/2}$ which at low frequencies decreases slowly with increasing resonance frequency, and an angular dependence of the form $\Delta H_{1/2} = A + B\cos^2\theta$.

The observation of a single, narrow ESR line is evidence that substantial narrowing of $\Delta H_{1/2}$ takes place. There are several interactions known to be present which, in the absence of narrowing, would lead to $\Delta H_{1/2}$ larger than observed. First, we discuss the contributions to $\Delta H_{1/2}$ without narrowing, and then comment on the narrowing. Similar considerations have been employed by Hughes and Soos.[33]

To begin, let us assume that the electronic spin states responsible for χ are localized to individual TCNQ molecules. Three of the contributions to $\Delta H_{1/2}$ are broadening by longitudinal relaxation (T_{1e}), the exchange and dipolar interactions of the electron spin with the nuclei, and the dipolar interaction with other electron spins. Anisotropy of the intrachain exchange is not considered for reasons given near the end of this section.

For an estimate of the importance of T_{1e} to the linewidth, we compare $T_{1e} \simeq 1.0$ μs at 295 MHz and 0.3 K (Fig. 4), $T_{2e} \simeq 0.67$ μs at 280 MHz and 0.3 K (Fig. 5), and the inverse linewidth $(\gamma_e \Delta H_{1/2})^{-1} = 0.32$ μs at 280 MHz and 0.3 K (Fig. 5). The fact that T_{2e} and $(\gamma_e \Delta H_{1/2})^{-1}$ are clearly less than T_{1e} shows that although some of the linewidth is caused by longitudinal relaxation, a substantial part of it must come from spin processes which do not cause longitudinal relaxation.

We can estimate the linewidth due to the electron dipole-dipole interaction by considering quinolinium(TCNQ)$_2$ as a random, 3D, pseudodilute spin system.[33] By this we mean the dipolar width of free spins having the same χ as that actually measured. The measured ESR molar susceptibility (χ) is represented as a fraction (f) of a Curie susceptibility (χ_0): $\chi = f\chi_0$. The range of f for the samples considered here varies from approximately 0.5% at 30 mK to 3% at 10 K.[3] An average spin density (n_s) is calculated using the equation $n_s = f\rho N_A/M$ where N_A is Avogadro's number, M is the molecular weight, and ρ is the mass density of quinolinium(TCNQ)$_2$.[29] The linewidth is then estimated using Anderson's result[34] for a dilute, random, nuclear spin system

$$\Delta H_{1/2} \simeq 3.8\gamma_e^2 \hbar n_s \tag{11}$$

and the substitutions $M = 538$ g/mole and $\rho = 1.4$ g/cm^3. This gives a linewidth (in the absence of narrowing) ranging from 1 G at 30 mK to 6 G at 10 K. It is much larger than what we measure and has the wrong T dependence. Clearly, this contribution to $\Delta H_{1/2}$ must be modified by narrowing.

We can also estimate a lower limit to the breadth of the structure caused by the hyperfine and dipolar interactions of an electron on an isolated TCNQ$^-$ ion. The hyperfine field seen by the electron from each of the protons[35] ($A/2\hbar\gamma_e$) is about 0.6 G and the average dipolar coupling[36] ($d/2\hbar\gamma_e$) is about 0.3 G. In addition, there is a contribution from the four ^{14}N nuclei. In solution, they show a scalar coupling[35] of about 1 G. This should be reduced in the solid by an amount difficult to evaluate since the electric field gradient of the noncubic environment introduces a quadrupolar interaction for the ^{14}N which can decrease the magnetic character of its spin states,[37] and therefore their magnetic interaction with the electron. A lower limit to the linewidth introduced by these electron-nuclear interactions on an isolated ion is $\Delta H_{1/2}$ for the envelope of the binomial distribution of the hyperfine field of the four protons, which is 3.3 G,[32] and, for the range of H and T covered in our experiments, independent of T. These properties are also at variance with our measurements of $\Delta H_{1/2}$ and point to narrowing of the interactions.

There are two kinds of effects expected to narrow $\Delta H_{1/2}$ from the above interactions: exchange narrowing[33,38,39] and electron delocalization.[32] Both are present in quinolinium(TCNQ)$_2$. The occurrence of large values of J is implicit in $\mathcal{H}_E$, and appreciable delocalization of the electrons is indicated by the frequency dependent transport[40,41] and magnetic properties of irradiated samples.[32]

Unfortunately, it is not currently possible to evaluate these factors quantitatively. There is not exchange narrowing theory for the special conditions (random 1D exchange with values both large and small compared to $k_B T$) of a REHAC. As far as the narrowing due to the delocalization of electrons is concerned, it has been pointed out elsewhere[32] that $\Delta H_{1/2}$ should be reduced as $n^{-1/2}$, where n is the

number of TCNQ molecules over which a spin state maintains coherence. It is much more difficult to evaluate the effect of delocalization on the electron-electron dipolar interaction in quinolinium(TCNQ)$_2$. More experimental and theoretical work is needed to clarify these issues.

There is another point to be made from the fact that a single, narrow line is observed in polycrystalline samples at all T. This means that the intrachain exchange coupling is extremely isotropic, i.e., of the pure Heisenberg form. If, on the contrary, there were any important anisotropy to this interaction, the magnetic splittings would, in the absence of exchange narrowing, depend on the orientation of H, and a polycrystalline sample would exhibit a power-pattern line shape with a width comparable to the magnitude of the anisotropy in J. Even when the effect of exchange narrowing is estimated using the standard formulas for uniform 1D and 3D antiferromagnets,[39] the anisotropy permitted in J is much less than 1%. According to recent calculations by Hirsch,[21] another manifestation of anisotropy in J would be removal of the low T divergence in χ. Experimentally,[42] the loss of this divergence occurs in the vicinity of 1–2 mK, and may be due to effects other than anisotropic exchange. Although it is difficult at present to develop this argument into a quantitative limit on the exchange anisotropy, qualitatively it is clear that the anisotropy is very small because the divergence is removed at such a low T.

An indication of the relative importance of electron-electron and electron-nuclear spin interactions to $\Delta H_{1/2}$ can be obtained by dividing the corresponding electron-free-induction decay into its reversible and irreversible parts. As an example, we use the 0.3 K values of T_{1e} (1.0 μs), T_{2e}, (0.67 μs), and $T_{2e}^{*} = 1/\gamma_e \Delta H_{1/2}$ (0.32 μs). We estimate the reversible part (w_r) of the free-induction decay rate to be $w_r = \gamma_e \Delta H_{1/2} - 1/T_{2e} \approx 1.6 \times 10^6$ s^{-1}, which is about half of the overall rate $\gamma_e \Delta H_{1/2} = 3.1 \times 10^6$ s^{-1}. Since w_r^{-1} is much shorter than the proton spin correlation time ($\sim$10 μs) inferred from the proton NMR absorption half-width we measure (4 G), the protons may be considered static on the scale of the electron spin correlation time. This means that the nuclear spin contribution to electron spin dephasing is nearly reversible. Let us make the reasonable assumption that it is the most important contribution to w_r. The anisotropy of the g tensor[6] should contribute about 10% (0.02 G) to $\Delta H_{1/2}$ for the conditions considered here. It then follows from the magnitude of w_r that the electron-nuclear spin interaction is responsible for about 40% of $\Delta H_{1/2}$. Also note that the irreversible part of the electron spin dephasing can be roughly divided between longitudinal and transverse (w_t) relaxation rates which are determined mainly by electron-electron interactions. By using the assumption that the rates are additive, we find $w_t = 1/T_{2e} - 1/T_{1e} \approx 0.5 \times 10^6$ s^{-1}. Thus, at 0.3 K, we estimate that about 40% of $\Delta H_{1/2}$ is due to electron-nuclear spin interactions, about 10% is due to the anisotropy of the g tensor, about 33% is due to Zeeman-exchange reservoir relaxation, and about 17% is due to transverse spin relaxation. The last two are probably driven by electron-electron dipolar interactions.

Now we comment briefly on the temperature and frequency dependence of $\Delta H_{1/2}$ indicated on Figs. 7–9. First, consider the increase in $\Delta H_{1/2}$ as T is decreased. (It has already been pointed out this behavior is the opposite of that estimated for the pseudodilute model without exchange narrowing.) We speculate that the mechanism responsible for this is a reduced exchange narrowing as T is decreased. The reduction comes about through the following steps. (a) For all the models we know of, $\Delta H_{1/2}$ decreases as J increases. (b) In a random exchange system, the magnetic properties are determined mainly by the spins for which $J \lesssim k_B T$, as indicated by the ECP model. (c) Hence, as T decreases, the effective J decreases and $\Delta H_{1/2}$ increases. Although this qualitative picture is a plausible explanation of the temperature dependence of $\Delta H_{1/2}$, it has not yet been quantified, and a direct comparison with the observed behavior [Eq. (1)] cannot be made.

The dependence of $\Delta H_{1/2}$ on ν (Fig. 9) is divided into two regions. Below 100 MHz, a logarithmic divergence [Eq. (2)] is observed. This follows qualitatively the behavior of T_{1e} and T_{2e} (Figs. 4 and 5) observed at higher ν. One factor which may contribute to this increase in $\Delta H_{1/2}$ is an increase in the Zeeman-exchange relaxation rate due to a low-energy divergence in the exchange reservoir density of states.[17] There are two comments to be made about the high ν deviation above Eq. (2). Since it has about the magnitude expected from the anisotropy of the g factor and the use of a powder sample discussed above, it is tempting to interpret it on that basis. In this case, it is expected that Eq. (2) holds for a single crystal to still higher ν. On the other hand, the 9.5 GHz measurement on a single crystal has a value of $\Delta H_{1/2}$ which just corresponds to the break from Eq. (2). This suggests that $\Delta H_{1/2}$ for a single crystal becomes independent of ν above 100 MHz. More work on this problem is required before the intrinsic behavior of $\Delta H_{1/2}$ above 100 MHz is known.

We conclude this section with a few brief remarks about the angular dependence of $\Delta H_{1/2}$ [Eqs. (3)–(5)]. The origin of this anisotropy must lie with one of the anisotropic spin interactions: electron-electron dipolar, electron-nuclear dipolar, or perhaps a weak anisotropic term in the exchange interaction. Even with exchange narrowing, the interaction responsible for $\Delta H_{1/2}$ should reflect the same symmetry seen in $\Delta H_{1/2}$, twofold rotation symmetry about all rotation axes and a maximum for H along the chain axis.

Unfortunately, for several reasons we are unable to tell if one of these interactions is primarily responsible for the angular dependence of $\Delta H_{1/2}$. The electron-electron dipolar width for a random pseudo-dilute model is isotropic. A maximum in $\Delta H_{1/2}$ for H directed along the chain axis would be expected for a strongly one-dimensional dipolar interaction, but not the angular dependence perpendicular to the chain axis [Eq. (3)].[39,43,44] In principle, an angular dependence of $\Delta H_{1/2}$ for H perpendicular to the chain axis can be caused by the electron-nuclear dipolar interaction. However, a simple model[13] using published electron densities at various sites on the TCNQ molecule does not explain it in detail. In particular, this calculation exhibits a maximum in $\Delta H_{1/2}$ for H perpendicular to the chain axis, rather than parallel to it. Finally, it is not known if there is a contribution to the anisotropy of $\Delta H_{1/2}$ from an anisotropy in T_{1e}.

V. CONCLUSIONS

We have reported measurements of the dynamic electron spin behavior in quinolinium$(TCNQ)_2$ using pulsed ESR over the frequency and temperature ranges 241–400 MHz and 0.03–4.2 K, as well as cw ESR over the ranges 10–290 MHz and 0.03–300 K. Below 0.1 K, the longitudinal spin relaxation has fast and a slow recovery components following disturbance from thermal equilibrium. Above 0.1 K, only the fast recovery is seen. The fast recovery, which is nearly independent of T and ν, is interpreted as magnetic cross relaxation between the Zeeman and exchange reservoirs. The observed characteristics are consistent with the identification of quinolinium $(TCNQ)_2$ as a REHAC. The slow relaxation component, which is strongly temperature dependent, is interpreted as relaxation of the Zeeman and exchange reservoirs together to the He bath. It is speculated that the rate of this process is limited by the Kapitza resistance. From cw measurements of the linewidth $\Delta H_{1/2}$, it is found that $\Delta H_{1/2}$ diverges logarithmically as T is reduced below 10 K and ν is reduced below 100 MHz. Also, the dependence of $\Delta H_{1/2}$ as a function of magnetic field orientation is reported for a single platelet sample. Insofar as possible, the role of electron-electron and electron-nuclear interactions in determining the relaxation rates have been indicated.

The series of experiments reported here indicate the need for much more theoretical and experimental work. Quantitative calculations of T_{1e} based on the Zeeman-exchange relaxation model of a REHAC should be carried out, along with calculations of the exchange-phonon relaxation characteristics. Further experimental studies should include work on samples treated to increase the surface to volume ratio to test for the importance of the Kapitza resistance in limiting energy transfer to the bath. Transient ESR measurements in the 1–20-GHz range should be performed to determine the relaxation characteristics under conditions in which the Zeeman splitting is large compared to $k_B T$. The importance of electron-nuclear interactions to $\Delta H_{1/2}$ should be investigated using samples in which these interactions have been changed by replacing deuterons with protons. Finally, direct relaxation measurements should be extended to samples whose disorder has been increased by neutron irradiation.[32]

ACKNOWLEDGMENTS

We thank R. Orbach and A. Lagendijk for discussions of several points related to the dynamics of 1D systems and are grateful to K. Holczer, A. J. Heeger, and N. Rysava for providing our samples. This material is based upon work supported by the National Science Foundation under Grants No. DMR 73-06712 and No. DMR 77-23577, and a grant from the UCLA Academic Senate Research Committee.

[1]L. N. Bulaevskii, A. V. Zvarykina, Y. S. Karimov, R. B. Lyobovskii, and I. F. Shchegolev, Zh. Eksp. Teor. Fiz. 35, 725 (1972) [Sov. Phys. JETP 35, 384 (1972)].
[2]J. Sanny and W. G. Clark, Solid State Commun. 35, 473 (1980).
[3]L. C. Tippie and W. G. Clark, Phys. Rev. B 23, 5846 (1981) (preceding paper).
[4]M. Miljak, J. Cooper, and G. Grüner, KFKI report (unpublished).
[5]M. Miljak, B. Korin, J. R. Cooper, K. Holczer, G. Grüner, and A. Jánossy, J. Magn. Magn. Mater. 15-18, 219 (1980).
[6]W. G. Clark, J. Hammann, J. Sanny, and L. C. Tippie, in *Proceedings of the 2nd International Conference on Quasi One-Dimensional Conductors, Dubrovnik, 1978,* edited by S. Barišić *et al.* (Springer, New York, 1979), p. 255.
[7]L. J. Azevedo and W. G. Clark, Phys. Rev. B 16, 3252 (1977).
[8]E. Ehrenfreund, S. Etemad, L. B. Coleman, E. F. Rybaczewski, A. F. Garito, and A. J. Heeger, Phys. Rev. Lett. 29, 269 (1972).
[9]L. J. Azevedo, W. G. Clark, E. O. McLean, and P. F. Seligmann, Solid State Commun. 16, 1267 (1975).
[10]F. Devreux, M. Nechtschein, and G. Grüner, Phys. Rev. Lett. 45, 53 (1980).
[11]R. G. Kepler, J. Chem. Phys. 39, 3259 (1963).
[12]L. C. Tippie and W. G. Clark, Bull. Am. Phys. Soc. 23, 431 (1978).

[13]L. C. Tippie (unpublished).
[14]W. G. Clark (unpublished).
[15]N. Bloembergen and S. Wang, Phys. Rev. 93, 72 (1954); P. M. Richards, *ibid.* 137, A1327 (1965).
[16]R. L. Garwin and A. Landesman, Phys. Rev. 133, A1503 (1964).
[17]W. G. Clark and L. C. Tippie, Phys. Rev. B 20, 2914 (1979).
[18]W. G. Clark, L. C. Tippie, G. Frossati, and H. Godfrin, J. Phys. (Paris) Suppl. 39, C6-1160 (1978).
[19]G. Theodorou and M. H. Cohen, Phys. Rev. Lett. 37, 1014 (1976); G. Theodorou, Phys. Rev. B 16, 2254, 2264, 2273 (1977).
[20]S. K. Ma, C. Dasgupta, and C. K. Hu, Phys. Rev. Lett. 43, 1434 (1979); C. Dasgupta and S. K. Ma, Phys. Rev. B 22, 1305 (1980).
[21]J. E. Hirsch and J. V. José, J. Phys. C Lett. 13, L53 (1980); Phys. Rev. B 22, 5339 (1980); J. E. Hirsch, *ibid.* 22, 5335 (1980).
[22]Z. G. Soos and S. R. Bondeson, Solid State Commun. 35, 11 (1980); S. R. Bondeson and Z. G. Soos, Phys. Rev. B 22, 1793 (1980).
[23]M. Goldman, *Spin Temperature and Nuclear Magnetic Resonance in Solids* (Oxford, London, 1970), Chap. 1.
[24]C. P. Slichter, *Principles of Magnetic Resonance,* 2nd ed. (Springer, Heidelberg, 1978).
[25]No explicit form for H_{ep} is specified in this paper.
[26]A knowledge of pulsed magnetic resonance comparable to that presented in Ref. 24 is assumed in this paper.
[27]Reference 23, Chap. 6.
[28]O. V. Lounasmaa, *Experimental Principles and Methods below 1 K* (Academic, London, 1974), pp. 263–270.
[29]H. Kobayashi, F. Marumo, and Y. Saito, Acta. Crystallogr. B 27, 373 (1971).
[30]Reference 28, pp. 270–274.
[31]By using $\lambda_{th} \simeq (5\Theta_D/T)$ Å, $T = 50$ mK, and the Debye temperature $\Theta_D \simeq 100$ K, we obtain $\lambda_{th} = 1$ μm.
[32]J. Sanny, G. Grüner, and W. G. Clark, Solid State Commun. 35, 657 (1980).
[33]R. C. Hughes and Z. G. Soos, J. Chem. Phys. 48, 1066 (1968).
[34]P. W. Anderson and P. R. Weiss, Rev. Mod. Phys. 25, 269 (1953).
[35]H. Haustein, K. P. Dinse, and K. Möbius, Z. Naturforsch. A 26, 1230 (1971).
[36]F. Devreux, A. Jeandey, M. Nechtschein, J. M. Fobre, and L. Giral, J. Phys. (Paris) 40, 671 (1979).
[37]T. P. Das and E. L. Hahn, in *Solid State Physics, Supplement 1, Nuclear Quadrupole Resonance Spectroscopy,* edited by F. Seitz and D. Turnbull (Academic, New York, 1958), Chap. 1.
[38]J. H. Van Vleck, Phys. Rev. 74, 1168 (1948).
[39]A. Lagendijk, Phys. Rev. B 18, 1322 (1979), and references cited therein.
[40]K. Holczer, G. Grüner, G. Mihály, and A. Jánossy, Solid State Commun. 31, 145 (1979).
[41]L. C. Tippie, G. Grüner, J. Sanny, and W. G. Clark, Bull. Am. Phys. Soc. 25, 217 (1980).
[42]H. M. Bozler, C. M. Gould, T. J. Bartolac, W. G. Clark, K. Glover, and J. Sanny, Bull. Am. Phys. Soc. 25, 217 (1980); H. M. Bozler, C. M. Gould, and W. G. Clark, Phys. Rev. Lett. 45, 1303 (1980).
[43]R. R. Bartkowski and B. Morosin, Phys. Rev. B 6, 4209 (1972).
[44]P. M. Richards, in *Local Properties at Phase Transitions, Proceedings of the International School of Physics "Enrico Fermi," Course LIX, Varenna, 1973,* edited by K. A. Müller and A. Rigamonti (North-Holland, Amsterdam, 1976), p. 539.